

**OPTICAL CONDUCTIVITY OF DOPED MANGANITES:
COMPARISON OF FERROMAGNETIC KONDO LATTICE MODELS
WITH AND WITHOUT ORBITAL DEGENERACY.**

Frank Mack and Peter Horsch

Max-Planck-Institut für Festkörperforschung,
Heisenbergstr. 1
D-70569 Stuttgart, Germany.

INTRODUCTION

The colossal magnetoresistance (CMR) of manganese oxides¹ and their transport properties are usually studied in the framework of the double exchange (DE) Hamiltonian or the more general ferromagnetic Kondo lattice model (KLM)². The essence of these models is the high-spin configuration of e_g -electron and t_{2g} -core electron spins due to a strong ferromagnetic Kondo exchange interaction $K \sim 1\text{eV}$. The kinetic energy in the partially filled e_g band is lowered when neighboring spins are aligned leading to a low-temperature ferromagnetic phase, while the high- T paramagnetic phase is disordered with a high resistivity. In these considerations the orbital degeneracy of the Mn e_g orbitals is usually neglected. Although this model provides an explanation of the phases necessary for a qualitative understanding of CMR, it has been stressed that the double exchange mechanism is not sufficient for a quantitative description.³

Doped manganites are characterized by strong correlations and the complex interplay of spin-, charge-, and orbital-degrees of freedom as well as the coupling to the lattice, e.g. via Jahn-Teller coupling.^{4,5} This complexity is directly evident from the large number of phases in a typical phase diagram. To quantify the different mechanisms it is helpful to analyze experiments where for certain parameters one or the other degree of freedom is frozen out. Important experiments in this respect are the very detailed investigations of the optical conductivity of $\text{La}_{1-x}\text{Sr}_x\text{MnO}_3$ by Okimoto *et al.*^{6,7} These experiments (see Fig. 1) show (a) a pseudogap in $\sigma(\omega)$ for temperatures above the Curie temperature T_c (paramagnetic phase) with $\sigma(\omega)$ essentially linear in ω , and (b) the evolution of a broad incoherent distribution in the range $0 \leq \omega < 1.0$ eV below T_c , which still grows at temperatures below $T_c/10$, where the magnetization is already close to saturation. Such a temperature dependence of $\sigma(\omega)$ over a wide energy region is quite unusual as compared with other strongly correlated electron systems near a metal-insulator phase boundary.⁶ Interestingly there is in addition a narrow

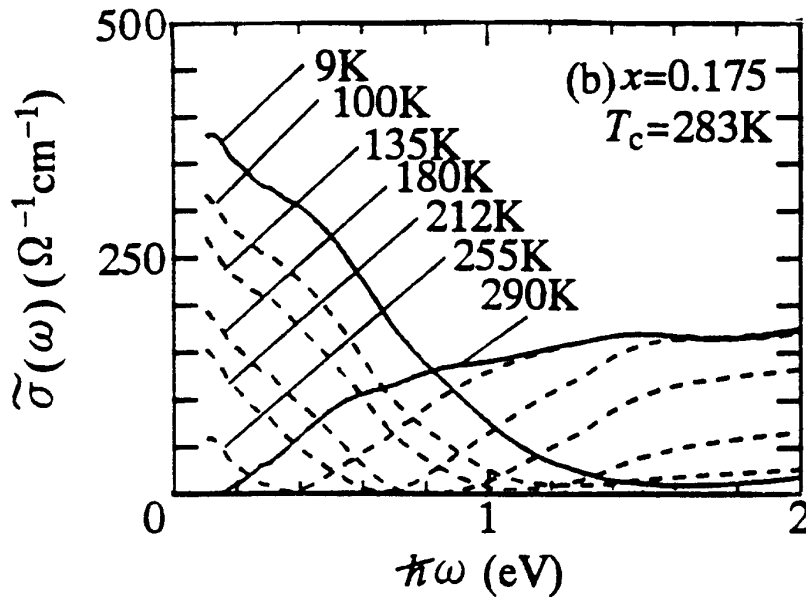


Figure 1: Temperature dependence of the optical conductivity of $\text{La}_{1-x}\text{Sr}_x\text{MnO}_3$ for $x = 0.175$ (reproduced from Okimoto *et al.*). A temperature independent background has been subtracted from the experimental data.

Drude peak with width of about 0.02 eV and little weight superimposed to the broad incoherent spectrum. That is, the motion of charge carriers is dominated by incoherent processes but there is also a coherent channel leading to a narrow Drude peak. In view of the large energy scale of 1 eV it is plausible that the orbital degeneracy is the source of this incoherent motion, since the spin degrees of freedom are essentially frozen out. Our study of the degenerate Kondo lattice model will support this point of view. Further optical studies for various 3D manganites⁸⁻¹⁰ as well as for the bilayer system $\text{La}_{1.2}\text{Sr}_{1.8}\text{Mn}_2\text{O}_7$ ¹¹ confirm the presence of the large incoherent absorption in the ferromagnetic state.

Although the importance of these experiments was recognized immediately, the few theoretical studies¹²⁻¹⁴ were confined to simplified models or approximations, thereby ignoring important aspects of the full many body problem.

The aim of this work is to show that in a model which accounts for the orbital degeneracy, yet assumes that the spins are fully polarized, the broad incoherent spectral distribution of $\sigma(\omega)$, its increase with decreasing temperature, as well as the order of magnitude of $\sigma(\omega)$ at small ω can be explained. Our calculation also accounts for a small and narrow Drude peak as observed by Okimoto *et al.* in the range $\omega < 0.05$ eV. This is a clear indication of coherent motion of charge carriers with small spectral weight, i.e. in a model where due to the orbital degeneracy incoherent motion is dominant.

We start our discussion with a generic Hamiltonian for the manganite systems, i.e. the ferromagnetic Kondo lattice model with degenerate e_g -orbitals, and derive for the spin-polarized case an effective model which contains only the orbital degrees of freedom. This orbital model consists of a hopping term between the same and different orbitals α and β on neighbor sites and an orbital interaction. Renaming $\alpha = \sigma$ where $\sigma = \uparrow$ or \downarrow the model maps on a generalized anisotropic t - J model. The usual t - J model known from the cuprates appears as a special case. Our derivation includes the 3-site hopping processes, which appear as a natural consequence of the strong coupling limit. Although such terms do not influence the orbital order for integer filling, they

are important for the proper description of transport properties in the doped systems.
17–20

Because of the complexity of the orbital model we present here a numerical study of the orbital correlations and of the frequency dependent conductivity.²¹ Although there exist studies of the interplay of orbital and spin order at integer filling for LaMnO₃,^{22,23} the effect of doping has not been considered so far. The finite temperature diagonalization^{24,25} serves here as an unbiased tool to study the optical conductivity. The change of orbital correlations as function of doping and temperature is investigated by means of an *optimized orbital basis* (OOB).²¹

Furthermore we present results for the KLM *without* orbital degeneracy which clearly show that this model fails to explain the broad incoherent $\sigma(\omega)$ spectra observed in the ferromagnetic phase as $T \rightarrow 0$.^{6,7} The KLM would instead lead to a sharp Drude absorption because of the ferromagnetic alignment,¹⁵ i.e. to spinless fermion behavior in the low-temperature limit. This underlines the importance of the e_g orbital degeneracy, although there are alternative proposals invoking strong electron-phonon coupling and lattice polaron formation^{4,3,16} to explain the incoherency of the absorption.

MODELS

We start from the generic ferromagnetic Kondo lattice model for the manganites, where the Mn e_g -electrons are coupled to core spins \vec{S}_i (formed by the t_{2g} orbitals) and a local repulsion U between the electrons in the two e_g orbitals:

$$H = H_{band} + H_{int} + H_{Kondo}. \quad (1)$$

H_{band} describes the hopping of e_g -electrons between sites i and j , H_{int} the interaction between e_g electrons and H_{Kondo} the coupling of e_g -spins and t_{2g} -core spins. The e_g electrons to have two-fold orbital degeneracy labelled by a Roman index (a,b) and two fold spin degeneracy labelled by a Greek index (σ, σ'). Explicitly,

$$H_{band} = \sum_{i\alpha\sigma} E_i^a d_{i\alpha\sigma}^\dagger d_{i\alpha\sigma} + \sum_{\langle \mathbf{i} \mathbf{j} \rangle ab\sigma} (t_{ij}^{ab} d_{i\alpha\sigma}^\dagger d_{j\beta\sigma} + H.c.). \quad (2)$$

The hopping matrix elements t_{ij}^{ab} form a real symmetric matrix whose form depends on the choice of basis in orbital space and the direction of the $\mathbf{i} - \mathbf{j}$ bond. For the present study we shall use $|x\rangle \sim x^2 - y^2$ and $|z\rangle \sim (3z^2 - r^2)/\sqrt{3}$ as basis for the e_g orbitals. From the Slater-Koster rules follows^{26–28}:

$$t_{ij\parallel x/y}^{ab} = -\frac{t}{4} \begin{pmatrix} 1 & \mp\sqrt{3} \\ \mp\sqrt{3} & 3 \end{pmatrix}, \quad t_{ij\parallel z}^{ab} = -t \begin{pmatrix} 1 & 0 \\ 0 & 0 \end{pmatrix}, \quad (3)$$

which allows for inter-orbital hopping in the xy -plane, where the upper (lower) sign distinguishes hopping along x and y direction. The hopping matrix elements are defined in terms of the double exchange t of $d_{3z^2-r^2}$ orbitals along the c -axis. Here $t = V_{dp\sigma}^2 / \Delta\epsilon_{dp}$ is determined by the Mn- d O- p hybridisation $V_{dp\sigma}$ and the corresponding level splitting $\Delta\epsilon_{dp}$. All matrix elements are negative except t^{xz} along x -direction, which is positive. The level splitting $\Delta E_i = E_i^z - E_i^x$ can be controlled by uniaxial pressure or in the case of layered compounds even with hydrostatic pressure.²⁹ We shall focus here on the orbital degenerate case, i.e. $\Delta E_i = 0$, however we will keep the orbital energy term for the derivation of the orbital model.

The large local electron-electron repulsion U is responsible for the insulating behavior in the case of integer band-filling

$$H_{int} = \sum_{\mathbf{ia}} U_a n_{\mathbf{ia}\uparrow} n_{\mathbf{ia}\downarrow} + U_{ab} \sum_{\mathbf{i}} n_{\mathbf{ia}} n_{\mathbf{ib}} + J_{ab} \sum_{\mathbf{i}\sigma\sigma'} d_{\mathbf{ia}\sigma}^\dagger d_{\mathbf{ib}\sigma'}^\dagger d_{\mathbf{ia}\sigma'} d_{\mathbf{ib}\sigma}. \quad (4)$$

Here U_a , U_{ab} and J_{ab} are the intra- and inter-orbital Hubbard and exchange interactions, respectively. The relevant valences of Mn are Mn^{3+} ($S=2$) and Mn^{4+} ($S=3/2$) as was pointed out already by Zener.² The Hamiltonian $H_{band} + H_{int}$ was considered by Zaanen and Oleś who showed that in general rather complex effective Hamiltonians result for transition metal ions with partially filled d shell near orbital degeneracy.³⁰ Here a simplified approach is preferred, with the t_{2g} electrons of Mn ions forming core spins of $S = 3/2$, and thus we restrict the electron interactions in H_{int} to the e_g bands.

Even in the case with local orbital degeneracy there is one lower Hubbard band which is partially filled in the case of hole doping. With one e_g -electron per site these systems are Mott-insulators. Although the Jahn-Teller splitting can lead to a gap in the absence of U , it is not the primary reason for the insulating behavior for integer filling.³¹

The interaction of itinerant electrons with the ($S=3/2$) core spins is given by

$$H_{Kondo} = -K \sum_{\mathbf{ia}\sigma\sigma'} \vec{S}_{\mathbf{i}} \cdot d_{\mathbf{ia}\sigma}^\dagger \vec{\sigma}_{\sigma\sigma'} d_{\mathbf{ia}\sigma'} \quad (5)$$

leading to parallel alignment of the d -electron spin with the core-spin $\vec{S}_{\mathbf{i}}$. Since the d -electron kinetic energy is favored by a parallel orientation of neighboring spins the ground state becomes ferromagnetic.²

In the low-temperature ferromagnetic phase we may introduce an effective Hamiltonian which contains only the orbital degrees of freedom assuming a fully spin-polarized ferromagnet. The spin degrees of freedom can also be eliminated by high magnetic fields. This opens the possibility to investigate the orbital order independent of the spin degrees of freedom, and to shed light on the nontrivial question how the orbital order is changed upon doping with e_g -electrons or holes.

The resulting model has similarities to the t - J model, where the spin-indices σ and σ' are now orbital indices. To stress the difference we use for the orbital indices the letters a, b and α, β . Unitary transformation $H_{orb} = e^{-S} H e^{S32}$ and the restriction to states without double occupancy leads to the *orbital* t - J model which has the following structure:

$$H_{orb} = \sum_{\mathbf{ia}} E_a^i \tilde{d}_{\mathbf{ia}}^\dagger \tilde{d}_{\mathbf{ia}} + \sum_{\langle \mathbf{ij} \rangle ab} (t_{\mathbf{ij}}^{ab} \tilde{d}_{\mathbf{ia}}^\dagger \tilde{d}_{\mathbf{jb}} + H.c.) + H'_{orb}. \quad (6)$$

with the constraint that each site can be occupied by at most one electron, i.e. $\tilde{d}_{\mathbf{ia}}^\dagger = d_{\mathbf{ia}}^\dagger (1 - n_{\mathbf{i}\bar{a}})$. Here and in the following the index \bar{a} denotes the orthogonal e_g orbital with respect to orbital a . The orbital interaction H'_{orb} follows as a consequence of the elimination of doubly occupied sites with energy $U \sim U_{ab} - J_{ab}$.²¹

$$H'_{orb} = -\frac{1}{2} \sum_{\mathbf{j}\mathbf{u}\mathbf{u}'} \sum_{\alpha\beta} t_{\mathbf{j}+\mathbf{u}\mathbf{j}}^{\alpha\beta} t_{\mathbf{j}\mathbf{j}+\mathbf{u}'}^{ba} \left(\frac{1}{U + E_{\mathbf{j}}^\beta - E_{\mathbf{j}+\mathbf{u}}^\alpha} + \frac{1}{U + E_{\mathbf{j}}^b - E_{\mathbf{j}+\mathbf{u}'}^a} \right) \left[\delta_{\beta,b} \tilde{d}_{\mathbf{j}+\mathbf{u}\alpha}^\dagger \tilde{d}_{\mathbf{j}\beta}^\dagger \tilde{d}_{\mathbf{j}\bar{\beta}} \tilde{d}_{\mathbf{j}+\mathbf{u}'a} - \delta_{\beta,\bar{b}} \tilde{d}_{\mathbf{j}+\mathbf{u}\alpha}^\dagger \tilde{d}_{\mathbf{j}\bar{\beta}}^\dagger \tilde{d}_{\mathbf{j}\beta} \tilde{d}_{\mathbf{j}+\mathbf{u}'a} \right]. \quad (7)$$

Here $\mathbf{u}, \mathbf{u}' = (\pm a, 0)$ or $(0, \pm a)$ are lattice unit vectors. The orbital interaction $H'_{orb} = H'_{orb}^{(2)} + H'_{orb}^{(3)}$ consists of two types of contributions: (i) 2-site terms ($\mathbf{u} = \mathbf{u}'$), i.e. similar to the Heisenberg interaction in the standard t - J model, yet more complex because

of the nonvanishing off-diagonal t^{ab} , and (ii) 3-site hopping terms ($\mathbf{u} \neq \mathbf{u}'$) between second nearest neighbors. In the half-filled case, i.e. one e_g -electron per site, only the 2-site interaction is operative and may induce some orbital order. In the presence of hole doping, i.e. for less than one e_g -electron per site, both the kinetic energy and the 3-site contributions in H'_{orb} lead to propagation of the holes and to a frustration of the orbital order.

The complexity of the model can be seen if we express the orbital interaction H'_{orb} in terms of pseudospin operators $T_i^z = \frac{1}{2}(n_{ia} - n_{ib})$, $T_i^+ = \tilde{d}_{ia}^\dagger \tilde{d}_{ib}$ and $T_i^- = \tilde{d}_{ib}^\dagger \tilde{d}_{ia}$. where $a = \uparrow$ and $b = \downarrow$ denote an orthogonal orbital basis in the e_g -space. To be specific we shall assume here $a(b) = z(x)$. Keeping only the two-site contributions, i.e. $\mathbf{u} = \mathbf{u}'$, one obtains an anisotropic Heisenberg Hamiltonian for the orbital interactions:

$$\begin{aligned}
H'_{orb}{}^{(2)} = -\frac{2}{U} \sum_{\langle ij \rangle} & \left[(t_{ij}^{aa^2} + t_{ij}^{bb^2}) \left(\frac{1}{4} n_i n_j - T_i^z T_j^z \right) - t_{ij}^{aa} t_{ij}^{bb} (T_i^+ T_j^- + T_i^- T_j^+) \right. \\
& + (t_{ij}^{ab^2} + t_{ij}^{ba^2}) \left(\frac{1}{4} n_i n_j + T_i^z T_j^z \right) - t_{ij}^{ab} t_{ij}^{ba} (T_i^+ T_j^+ + T_i^- T_j^-) \\
& \left. - (t_{ij}^{aa} t_{ij}^{ab} - t_{ij}^{bb} t_{ij}^{ba}) (T_i^z T_j^+ + T_i^z T_j^-) - (t_{ij}^{aa} t_{ij}^{ba} - t_{ij}^{bb} t_{ij}^{ab}) (T_i^+ T_j^z + T_i^- T_j^z) \right]. \quad (8)
\end{aligned}$$

The orbital interaction $H'_{orb}{}^{(2)}$ is equivalent to that studied by Ishihara *et al.*^{22,29} Since we are interested here in the effect of holes on the orbital order we will generally base our study on H'_{orb} (7) which includes the 3-site hopping processes as well.

We note that in the special case $t_{ij}^{ab} = \delta_{ab} t$ and $E_i^a = 0$ equations (6) and (7) are identical to the usual t - J model (with $J = 4t^2/U$ and including 3-site processes). For the orbital model we shall adopt the same convention for the orbital exchange coupling, i.e. $J = 4t^2/U$.

The orbital degrees of freedom in combination with strong correlations (i.e. no doubly occupied sites are allowed) is expected to lead to incoherent motion of holes, although quasiparticle formation with reduced spectral weight is a plausible expectation on the basis of what is known about the usual t - J model.

In this paper we focus on the orbital degenerate case with $E_i^a = E_i^b = 0$. A detailed study of the influence of a finite level splitting will be presented elsewhere.

OPTICAL CONDUCTIVITY

We study the charge transport by calculating the optical conductivity

$$\sigma_0(\omega) = 2\pi e^2 D_c \delta(\omega) + \sigma(\omega). \quad (9)$$

The frequency dependent conductivity consists of two parts, the regular finite frequency absorption $\sigma(\omega)$ and the δ -function contribution which is proportional to the charge stiffness D_c ^{35,33}. The latter vanishes in insulators. This contribution is broadened into a usual Drude peak in the presence of other scattering processes like impurities which are not contained in the present model. The finite frequency absorption (or regular part) $\sigma(\omega)$ is determined by the current-current correlation function using the Kubo formula

$$\sigma(\omega) = \frac{1 - e^{-\omega/T}}{N\omega} \text{Re} \int_0^\infty dt e^{i\omega t} \langle j_x(t) j_x \rangle. \quad (10)$$

For the derivation of the current operator we introduce twisted boundary conditions via Peierls construction

$$t_{\mathbf{j}+\mathbf{u}\mathbf{j}}^{ab}(\vec{A}) = t_{\mathbf{j}+\mathbf{u}\mathbf{j}}^{ab} \exp\left(-i\frac{e}{\hbar} \int_{\mathbf{j}}^{\mathbf{j}+\mathbf{u}} \vec{A}(x) d\vec{x}\right). \quad (11)$$

Assuming $\vec{A} = (A_x, A_y, 0)$ we obtain from the kinetic energy operator the x-component of the current operator $j_x = \partial H(A_x)/\partial A_x$:

$$j_x^{(1)} = -ie \sum_{\mathbf{j}+\mathbf{u}ab} t_{\mathbf{j}+\mathbf{u}\mathbf{j}}^{ab} u_x \tilde{d}_{\mathbf{j}+\mathbf{u}a}^\dagger \tilde{d}_{\mathbf{j}b}. \quad (12)$$

An additional contribution follows from the 3-site term in Eq.(6)

$$j_x^{(3)} = \frac{ie}{2U} \sum_{\mathbf{j}\mathbf{u}\mathbf{u}'} \sum_{ab\alpha\beta} t_{\mathbf{j}+\mathbf{u}\mathbf{j}}^{\alpha\beta} t_{\mathbf{j}\mathbf{j}+\mathbf{u}'}^{ba} (u_x - u'_x) O_{ba}^{\alpha\beta}(\mathbf{j}, \mathbf{u}, \mathbf{u}'), \quad (13)$$

$$O_{ba}^{\alpha\beta} = \delta_{\beta,b} \tilde{d}_{\mathbf{j}+\mathbf{u}\alpha}^\dagger \tilde{d}_{\mathbf{j}\bar{\beta}} \tilde{d}_{\mathbf{j}+\mathbf{u}'a} - \delta_{\beta,\bar{b}} \tilde{d}_{\mathbf{j}+\mathbf{u}\alpha}^\dagger \tilde{d}_{\mathbf{j}b} \tilde{d}_{\mathbf{j}+\mathbf{u}'a},$$

where the expression $O_{ba}^{\alpha\beta}(\mathbf{j}, \mathbf{u}, \mathbf{u}')$ is an abbreviation for the operator within the last brackets of Eq.(6).

We stress here that the orbital order in the undoped case is determined exclusively by the (two-site) orbital interaction (7), while the 3-site processes in (6) only contribute in the doped case. Nevertheless the motion of holes and transport in general is influenced in a significant way by the 3-site current operator $j_x^{(3)}$. In fact from studies of the t - J model it is known that $\sigma(\omega)$ is not only quantitatively but even qualitatively changed by these terms.^{18,19} Although the 3-site terms are usually ignored in studies of the t - J model they are an important part of the strong coupling model and should not be dropped in studies of the conductivity. One of the aims in our study of the orbital model is to analyse the effect of these 3-site terms in the model.

The charge stiffness D_c can be determined in two ways: (a) using Kohn's relation,³⁵ or (b) via the optical sum rule which relates the integrated spectral weight of the real part of the conductivity to the average kinetic energy:

$$\int_{-\infty}^{\infty} \sigma_0(\omega) d\omega = -\frac{\pi e^2}{N} \langle H_{xx}^{kin} \rangle. \quad (14)$$

Here H^{kin} contains two contributions: (a) the usual kinetic energy $\sim t$ (5) and (b) the 3-site hopping processes $\sim t^2/U$ in Eq. (6). The case with off-diagonal hopping considered here is a generalization of the sum rules for the t - J model³⁶ and for the t - J model including 3-site terms.^{18,20} Together with (8) this implies

$$D_c = -\frac{1}{2N} \langle H_{xx}^{kin} \rangle - \frac{1}{\pi e^2} \int_{0^+}^{\infty} \sigma(\omega) d\omega. \quad (15)$$

In the following we shall use $D_c = S - S_\omega$ as abbreviation for this equation, where S denotes the sum rule expression and S_ω the finite frequency absorption.

FINITE TEMPERATURE LANCZOS METHOD (FTLM)

For the calculation of $\sigma(\omega)$ we use a generalization of the exact diagonalization technique for finite temperature developed by Jaklič and Prelovšek.²⁴ In this approach the trace of the thermodynamic expectation value is performed by a Monte-Carlo sampling. The current-current correlation function in (9):

$$C(\omega) = Re \int_0^\infty dt e^{i\omega t} \langle j_x(t) j_x \rangle. \quad (16)$$

can be rewritten by introducing a complete set of basis functions $|r\rangle$ for the trace, and eigenfunctions $|\Psi_j^r\rangle$ and $|\tilde{\Psi}_j^r\rangle$ of H with eigenvalues E_i^r and \tilde{E}_j^r (here r is an irrelevant label, which will get its meaning below):

$$C(\omega) \approx \frac{\pi}{Z} \sum_{r=1}^R \sum_{i,j=1}^M e^{-\beta E_i^r} \langle r | \Psi_i^r \rangle \langle \Psi_i^r | j_x | \tilde{\Psi}_j^r \rangle \langle \tilde{\Psi}_j^r | j_x | r \rangle \delta(\omega + E_i^r - \tilde{E}_j^r) \quad (17)$$

with

$$Z \approx \sum_{r=1}^R \sum_{i=1}^M e^{-\beta E_i^r} |\langle r | \Psi_i^r \rangle|^2. \quad (18)$$

These expressions are exact if one uses complete sets. The FTLM is based on two approximations when evaluating Eqs.(17) for $C(\omega)$ and (18) for the partition function Z : (1) The trace is performed over a restricted number R of random states $|r\rangle$, and (2) the required set of eigenfunctions of H is generated by the Lanczos algorithm starting from the initial states $|\Phi_0^r\rangle = |r\rangle$ and $|\tilde{\Phi}_0^r\rangle = j_x |r\rangle / \sqrt{\langle r | j_x^2 | r \rangle}$, respectively. The latter procedure is truncated after M steps and yields the relevant intermediate states for the evaluation of $C(\omega)$.

Detailed tests²⁴ have shown that the results get very accurate already if $R, M \ll N_0$, where N_0 is the dimension of the Hilbert space. The computational effort is significantly reduced because only matrices of dimension $M \times M$ have to be diagonalized, i.e. much smaller than the dimension $N_0 \times N_0$ of the full Hamiltonian H . In practice typical dimensions are $R = 100$ and $M = 100$.

A complication in the case of the orbital t - J model is that T_{tot}^z does not commute with the Hamiltonian H_{orb} (6). Therefore the calculations for the orbital model are restricted to smaller clusters than in the t - J case, where different S_{tot}^z subspaces can be treated separately.

RESULTS

Kondo-Lattice Model without Orbital Degeneracy

We begin our discussion of the frequency dependent conductivity with results for the *single orbital Kondo-lattice model* excluding double occupancy

$$H = - \sum_{ij\sigma} t_{ij} \tilde{d}_{i\sigma}^\dagger \tilde{d}_{j\sigma} - J_H \sum_{i\sigma\sigma'} \vec{S}_i \cdot \tilde{d}_{i\sigma}^\dagger \vec{\sigma}_{\sigma\sigma'} \tilde{d}_{i\sigma}. \quad (19)$$

Nearest neighbor hopping $t_{ij} = t$ is assumed and the actual calculations were performed for $S = 1$ core spins for different doping concentrations x .

In Fig.2 the temperature dependence of the optical conductivity is shown for a chain at doping $x = 2/6$. The conductivity is given in dimensionless form $\sigma \rho_0$, where $\rho_0 = \hbar a / e^2$ sets the dimension of the resistivity in a 3D s.c. crystal structure with lattice constant a . At strong coupling $J_H \gg t$ the states of the model consist of a low-energy band corresponding to the $S + 1/2$ configurations, and of the exchange-split bands separated by an energy $\frac{3}{2} J_H$. The intraband transitions are shown in the large window. They give rise to an incoherent low-energy absorption extending up to the energy of the free carrier band-width $\sim 4t$. The spectrum of the high to low spin transitions is centered around $\omega \sim \frac{3}{2} J_H$ and is shown in the inset.

At low temperatures, however, when ferromagnetic correlations extend over the whole system, the low-energy spectrum is dominated by a narrow coherent peak at $\omega = 0$, and the interband transitions vanish. At $T = 0$ all weight is in the Drude peak

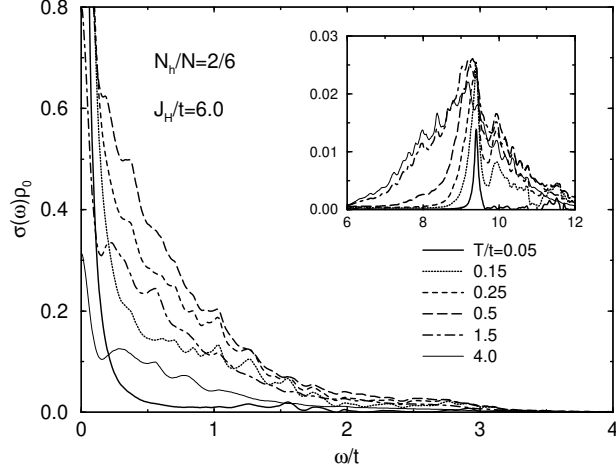


Figure 2: Frequency dependent conductivity $\sigma(\omega)$ of the *single orbital KLM* for a six site chain with two electrons and $J_H = 6t$ for different temperatures. Inset shows the spectrum of excitations to the exchange-split band. Note that for $T \rightarrow 0$ all spectral weight is in the Drude peak (From Jaklič, Horsch and Mack¹⁵).

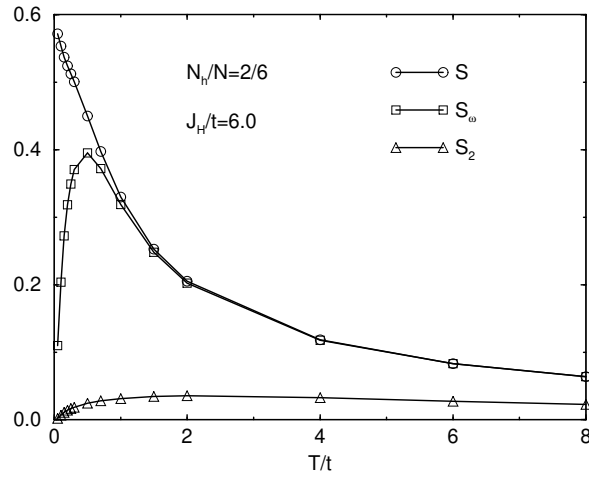


Figure 3: Temperature dependence of the kinetic energy and of the optical spectral weights of the ferromagnetic *Kondo-lattice model in the absence of orbital degeneracy* for a 6 site chain with two holes. Here $S = \langle H_{xx}^{kin} \rangle / 2Nt$ and $S_w = \int \sigma(\omega) d\omega / \pi e^2 t$. The spectral weight of the interband optical transitions into low-spin states is measured by $S_2 = \int \sigma_2(\omega) d\omega / \pi e^2 t$.

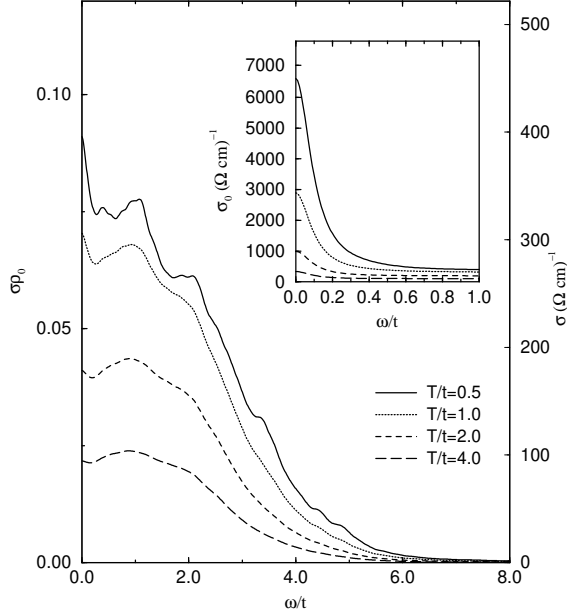


Figure 4: Optical conductivity $\sigma(\omega)$ calculated for the *orbital t-J model* for a N=10 site plane with $N_e=8$ electrons and $J=0.25t$ ($U=16t$) at different temperatures. The calculation includes the 3-site terms. The inset shows the optical conductivity $\sigma_0(\omega)$ including the Drude-part. The spectra were broadened with $\Gamma=0.1t$.

(see Fig.3). As the temperature is increased the spectral weight is transferred from the coherent part to the broad incoherent spectrum and to the exchange-split excitations. This clearly shows that the model without orbital degeneracy does not explain the anomalous absorption in the ferromagnetic state of manganites (Fig.1).

Optical Conductivity for the Orbital *t-J* Model

Typical results for the frequency and temperature dependence of $\sigma(\omega)$ for a two-dimensional 10-site cluster with 2 holes, i.e. corresponding to a doping concentration $x = 0.2$, are shown in Fig. 4 with and Fig. 5 without 3-site hopping terms, respectively. The $\sigma(\omega)$ spectra are bell-shaped and increase with decreasing temperature. The width of the distribution measured at half-maximum is $\omega_{1/2} \sim 2.5t$ and is essentially independent of temperature. Calculations for a 3D cluster yield a rather similar $\sigma(\omega)$ distribution with a slightly larger value for the width $\omega_{1/2} \sim 3.5t$.

If we compare this latter (3D) value with $\omega_{1/2}^{exp} \sim 0.7$ eV found from the data of Okimoto *et al.* (for $x = 0.175$ and $T = 9K$), we obtain an experimental estimate for the parameter t : $t^{opt} \sim 0.2$ eV. For comparison a rough theoretical estimate based on Harrison's solid state table yields $t = V_{dp\sigma}^2/\Delta\epsilon \sim 0.4$ eV. Hence the orbital *t-J* model explains in a natural way the ~ 1 eV energy scale of the incoherent absorption in the experiments. Although $\sigma(\omega)$ shows the anomalous increase with decreasing temperature, we do not claim here that the orbital model accounts for the full temperature dependence in the ferromagnetic phase ($T < T_c$). The description of the complete T -dependence certainly requires the analysis of the degenerate-orbital KLM, i.e. the additional inclusion of the spin degrees of freedom. Yet we believe that the results can be compared with the data by Okimoto *et al.* in the low- T limit, i.e. in the regime where the magnetization is saturated.

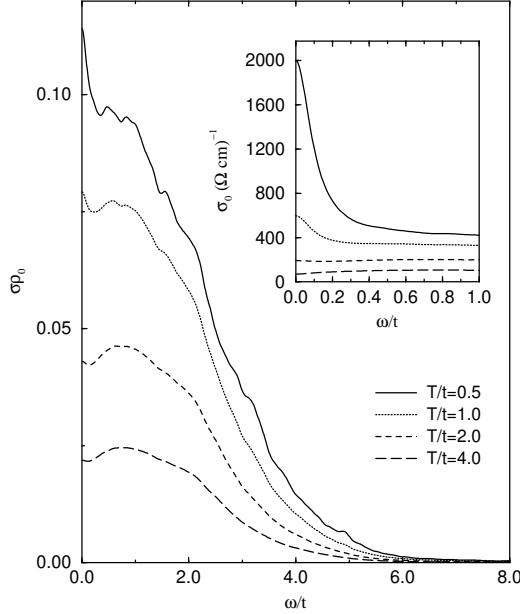


Figure 5: Optical conductivity as in Fig.4 but without 3-site contributions. Due to the stronger incoherence there is a smaller Drude peak (inset) and a smaller DC-conductivity. (From Horsch, Jaklič and Mack²¹).

To compare with experimental data we present the conductivity in dimensionless form and with the proper dimensions of a 3D conductivity, assuming that the 3D system is formed by noninteracting layers. For a cubic lattice $\rho_0 = \hbar a/e^2$. If we consider $\text{La}_{1-x}\text{Sr}_x\text{MnO}_3$ with lattice constant $a = 5.5 \text{ \AA}$ and $\hbar/e^2 = 4.11\text{K}\Omega$ we obtain $\rho_0 = 0.23 \cdot 10^{-3} \text{ \Omega cm}$. Hence the low frequency limit of the regular part of the conductivity $\sigma(\omega \rightarrow 0) = \sigma_0^{inc} \sim 0.3-0.4 \cdot 10^3 (\text{ \Omega cm})^{-1}$. This is consistent with the order of magnitude for the low frequency limit of the incoherent part of the $\sigma(\omega)$ data of Okimoto *et al.* for $\text{La}_{1-x}\text{Sr}_x\text{MnO}_3$ $\sigma_0^{inc} \sim 0.4 \cdot 10^3 (0.3 \cdot 10^3) (\text{ \Omega cm})^{-1}$ for the doping concentrations $x = 0.175 (0.3)$, respectively, at $T = 10\text{K}$.

Hence we conclude that besides the energy scale also the absolute value of the incoherent part of the experimental $\sigma(\omega)$ spectrum is consistent with the orbital model. We stress that the value (order of magnitude) of σ_0^{inc} is essentially fixed by the conductivity sum rule and the scale $\omega_{1/2}$, as long as the conductivity is predominantly incoherent. The insets in Fig.4 and 5 show $\sigma_0(\omega)$, Eq.(9), with the Drude absorption at low frequency included, where we used an ad hoc chosen parameter $\Gamma = 0.1t$ to broaden the δ -function. This value corresponds to the experimental width $\Gamma \sim 0.02 \text{ eV}$ taken from the (small) Drude peak observed by Okimoto *et al.*.⁷ While our model yields the weight of the Drude peak D_c , it does not give Γ , which is due to extrinsic processes (e.g. scattering from impurities and grain boundaries). The charge stiffness D_c together with Γ determines the DC-conductivity.

Adopting the experimental estimate for Γ we find for the example in Fig.4 (inset) for the low temperature DC-conductivity $\sigma_{DC} \sim 6.5 \cdot 10^3 (\text{ \Omega cm})^{-1}$ and for the resistivity $\rho \sim 0.15 \cdot 10^{-3} \text{ \Omega cm}$, respectively. For comparison, the experimental range of resistivities is e.g. $0.1 - 1.0 \cdot 10^{-3} \text{ \Omega cm}$ in the ferromagnetic metallic phase of $\text{La}_{1-x}\text{Sr}_x\text{MnO}_3$ ³⁴. As we shall see below, the Drude weight and therefore the DC-conductivity depend considerably on the value of the exchange coupling J , and whether the 3-site hopping processes in the model are taken into account or not. These terms have a strong effect on

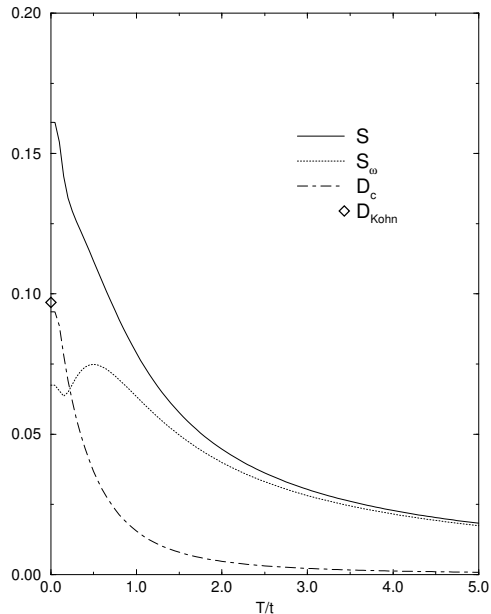


Figure 6: Temperature dependence of the kinetic energy S (solid line), the incoherent spectral weight S_ω (dotted) and the Drude weights D_c (dash-dotted line) and D_{Kohn} (diamond) for a $N=10$ site plane with $N_e=8$ electrons and $J=0.25t$ ($U=16t$) in units of $t/\rho_0 e^2$.

the coherent motion of charge carriers. After this discussion it should be clear, however, that the DC-conductivity at low temperatures is largely determined by extrinsic effects.

Figure 6 shows the temperature variation of the sum rule (kinetic energy), the finite frequency absorption S_ω and the Drude weight D_c for the model including the 3-site terms. Whereas at high temperature the sum rule is essentially exhausted by the finite frequency absorption $\sigma(\omega)$, we find at low temperatures a significant increase of the Drude weight. In this particular case D_c contributes about 40% to the sum rule at $T/t = 0.3$.

The conductivity data shown in Figs. 4 and 5 for $T/t > 0.5$ is characteristic for a 2D orbital liquid state, which is stabilized by thermal fluctuations. The significant increase of coherency in Fig. 6 below $T/t = 0.3$ is due to the onset of x^2-y^2 orbital order in the planar model (see discussion below). This ordering is characteristic for the 2D version of the orbital t - J model and does probably not occur in cubic systems for which an orbital liquid ground state was proposed.¹³ Therefore we consider the $T/t = 0.3$ data for D_c to be more appropriate for a comparison with the low-temperature 3D data than the $T = 0$ values, which are enhanced due to orbital order.

We have also calculated D_c for $T = 0$ using Kohn's relation³⁵

$$D_{Kohn} = \frac{1}{2N} \left. \frac{\partial^2 E_0(\Phi)}{\partial \Phi^2} \right|_{\Phi=\Phi_0}, \quad (20)$$

which yields a consistent value (Fig.6). Here $\Phi = eaA_\alpha/\hbar$ is the Peierls phase induced by the applied vector potential with component A_α . For the evaluation of Eq.20 we followed Ref.¹⁸ and first searched for the minimum of the ground state energy E_0 with respect to the vector potential,³⁷ and then calculated the curvature. Since this procedure is quite

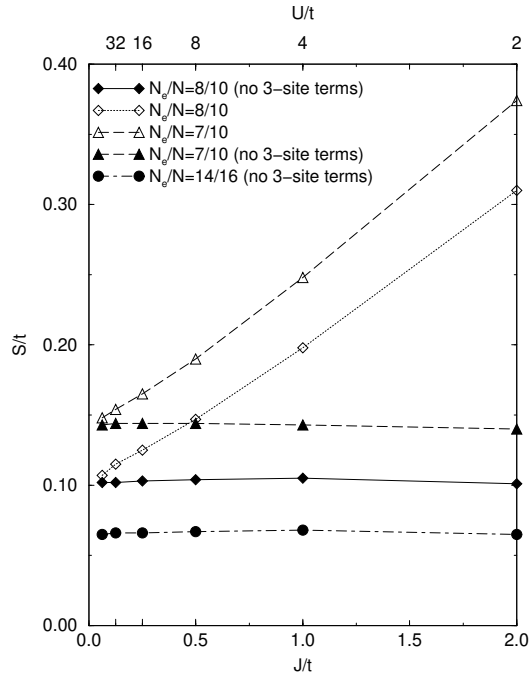


Figure 7: Kinetic energy S versus J for a $N=10$ site 2D cluster with $N_e=7$ and 8 electrons, with (full) and without (open symbols) the 3-site terms ($T/t = 0.3$), respectively. The dash-dotted line (circles) represents a 16 site cluster with $N_e=14$ and without 3-site terms (From Horsch, Jaklič and Mack²¹).

cumbersome, we have determined most of our D_c data via the sum rule. The resulting sets of data show systematic trends as function of J and doping.

From these results we expect in analogy with the t - J model that the single-particle electron Green's function is characterized by a pronounced quasiparticle peak to explain such a large fraction of coherent transport.

From Fig.6 we also see that the weight under $\sigma(\omega)$, i.e. S_ω , does not further increase for temperatures below $T = 0.5t$, although the temperature variation in Fig.4 seems to suggest a significant further increase towards lower temperatures. Conductivity data for $T < 0.5t$ is not shown in Figs. 4 and 5 because it shows pronounced discrete level structure, and probably requires larger clusters for a careful study. Nevertheless it appears that $\sigma(\omega)$ develops a pseudogap in the orbital ordered phase.³⁸ Integrated quantities on the other hand are much less influenced by such effects.

The Role of 3-Site Terms

In the following we wish to shed more light on the role of the 3-site processes in the orbital Hamiltonian and in the current operator. The importance of the 3-site term becomes particularly clear from the J -dependence of the sum rule S (Fig.7) and the charge stiffness D_c (Fig.8) taken at temperature $T/t = 0.3$. These low temperature values of S and D_c are approximately independent of the exchange parameter J in the absence of 3-site terms. A similar observation was made for the t - J model.^{39,18} Moreover one can see that the sum rule S is proportional to the doping concentration x for the 3 cases shown ($x=0.125, 0.2$, and 0.3). When 3-site terms are taken into account both S and D_c acquire a component which increases linearly with J . These general features are fully consistent with results for the t - J model.¹⁸

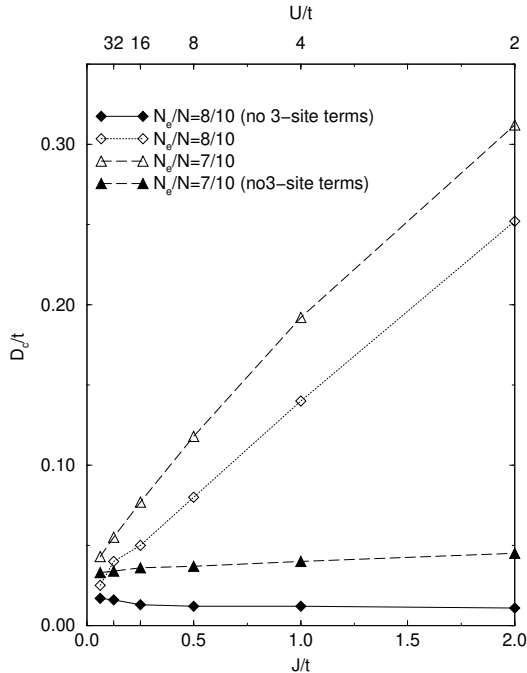


Figure 8: Drude weight D_c versus J calculated via the sum-rule (15) for a $N=10$ site planar cluster with $N_e=7$ and 8 e_g electrons, with and without the 3-site terms, respectively.

The change due to the 3-site terms is particularly large for the charge stiffness, which defines the weight of the low frequency Drude peak. The relative weight in the Drude peak D_c/S is shown in Fig. 8 as function of $J = 4t^2/U$. Small changes in J lead to considerable changes in the Drude weight and the coherent motion of carriers. For $J = 0.25$ (0.5) the 3-site terms lead to an increase of D_c by a factor of 3 (5), respectively, for the 8 electron case.

When we take the value $t \sim 0.2$ eV, which we determined from the comparison of $\sigma(\omega)$ with the experimental data, and $U \sim 3$ eV,²² we obtain $U/t \sim 15$ and $J/t = 4t/U \sim 0.25$ ($J = 0.05$ eV). For such a value for J we expect a relative Drude weight $D_c/S \sim 0.4$, which is larger than the experimental ratio $D_c/N_{eff} \sim 0.2$ found by Okimoto *et al.* for $x = 0.175$, identifying here the effective number of carriers N_{eff} ⁷ with S . The small value for D_c/N_{eff} found in the experiments suggests that J is not larger than the value estimated, otherwise we would expect a too large relative Drude weight. A larger value for U would also have the effect to reduce D_c . However, we have to stress here that certainly calculations on larger clusters must be performed, before possible finite size effects in D_c can be quantified.

Comparison with the standard t - J Model

It is interesting to compare these results for the orbital t - J model with those obtained for the usual t - J model describing the carrier motion in the copper-oxygen planes in high- T_c superconductors. We note that the t - J model is a special case of the orbital model with $t_{aa} = t_{bb}$ and $t_{ab} = 0$. Figures 9 and 10 show results for a 4×4 cluster with $N_h = 3$ holes. The results for $\sigma(\omega)$ show for both models a large incoherent absorption, which is bell-shaped in the case of the orbital model, while in the t - J case there is a continuous increase of $\sigma(\omega)$ as ω approaches zero. The temperature dependence of the sum rule, the incoherent and the Drude weight shown in Fig. 10 are quite similar for

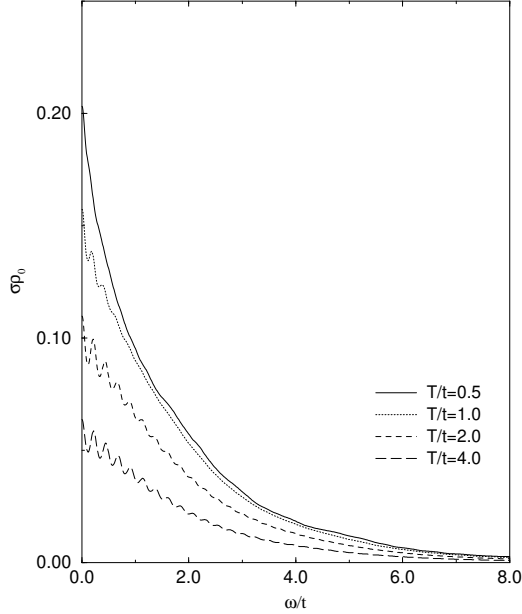


Figure 9: Optical conductivity for the *standard t-J model* ($t_{aa} = t_{bb} = t$ and $t_{ab} = 0$) at temperatures $T = 0.5, 1.0, 2.0$ and 4.0 which should be compared with the corresponding data for the orbital model. Here $N_h/N = 3/16$ and $J/t = 0.4$.

both models, with the important exception that the orbital model goes into the ordered phase at low temperatures ($T \leq 0.3$) which is accompanied by a marked increase of S and D_c (Fig.6). A more detailed study of the T -dependence may be found in the review by Jaklič and Prelovšek.²⁵

Comparison with other Work

The optical conductivity for the orbital non-degenerate Kondo lattice model was studied by Furukawa using the dynamical mean-field approximation.¹² An important result of this calculation is, that the weight of intraband excitations within the lower exchange-split band should be proportional to the normalized ferromagnetic magnetization M/M_{sat} . Experimentally, however, $N_{eff}(\sim S)$ is still increasing when temperature is lowered even though M is already saturated. This contradiction to the prediction of the simple double-exchange model implies that some other large-energy-scale scattering mechanism survives at low temperature, where the spins are frozen.⁷ The dynamical mean field theory yields one low energy scale, and not two, i.e. there is no Drude peak plus incoherent structure.

Shiba and coworkers *et al.*¹⁴ approached the problem from the band picture. They analysed the noninteracting two-band model (2) (i.e. without constraint) and argued that the interband transitions within the e_g orbitals may explain the anomalous absorption in the ferromagnetic phase of $\text{La}_{1-x}\text{Sr}_x\text{MnO}_3$. While the frequency range of the interband transition is found consistent with the anomalous absorption, the structure of $\sigma(\omega)$ differs. In particular the noninteracting model leads to $\sigma(\omega) \sim \omega$ for small ω . Moreover they calculated the ratio $S_\omega/D_c \sim 0.85$, i.e. there is more weight in the Drude peak than in the regular part of the conductivity $\sigma(\omega)$. This ratio is found to be rather insensitive to doping in the range $0.175 < x < 0.3$. This result differs considerably from the experimental data of Okimoto *et al.* where this ratio is about 4 for $x = 0.175$.

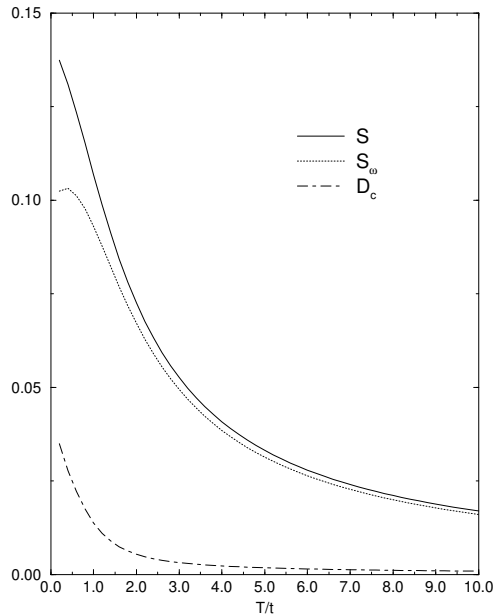


Figure 10: Temperature dependence of the kinetic energy S (solid line), the incoherent spectral weight S_ω (dotted) and the Drude weight D_c (dash-dotted line) for the t - J model. The data was calculated for a 2D system with 16 sites and 3 holes for $J/t=0.4$.

Orbital fluctuations in the ferromagnetic state and their effect on the optical conductivity were studied by Ishihara *et al.*¹³ using slave fermions coupled to bosonic orbital excitations. Ishihara *et al.* deal with the concentration regime $xt \gg J$, where the kinetic energy is expected to dominate the orbital exchange energy, and arrive at the conclusion that the quasi two-dimensional nature of the orbital fluctuations leads to an *orbital liquid* in (3D) cubic systems. The orbital disorder is treated in a static approximation in their work. The $\sigma(\omega)$ spectrum obtained by this approach for $T = 0.1t$ has a quite similar shape as the experimental spectrum at low temperature (with $\omega_{1/2} \sim 3t$), however, because of the assumed static disorder, there is no Drude component. A further problem with the orbital liquid, as noted by the authors, is the large entropy expected for the orbital disordered state which seems to be in conflict with specific heat measurements.⁴⁰

More recently a microscopic theory of the optical conductivity based on a slave boson parametrization which combines strong correlations and orbital degeneracy was developed by Kilian and Khaliullin⁴¹ for the ferromagnetic state at zero temperature. Their approach yields a highly incoherent spectrum due to the scattering of charge carriers from dynamical orbital fluctuations, and a Drude peak with strongly reduced weight. However $\sigma(\omega)$ is depressed at low frequency in this calculation for the orbital model and an additional electron-phonon mechanism is invoked to obtain results similar to the experimental spectral distribution. This theory further accounts for the small values of the specific heat and therefore supports the orbital liquid scenario for the ferromagnetic cubic systems.¹³

We would like to stress that the proposed orbital liquid state¹³ is a property of cubic systems, and not a property of the 2D or quasi-2D versions of the orbital model. In the planar model the cubic symmetry is broken from the outset and holes presumably cannot restore it. This is different from the physics of the t - J model, where holes restore the spin rotational symmetry (which is spontaneously broken in the antiferromagnetic

ordered phase), because this symmetry is respected by the t - J Hamiltonian in any dimension.

For a deeper understanding of the results for the optical conductivity, we shall analyse below the structure of the orbital correlations in the doped and undoped two-dimensional orbital model in detail.

DOPING DEPENDENCE OF ORBITAL CORRELATIONS

In the absence of holes the interaction (9) between orbital pseudo-spins will lead to an orbital order below a certain temperature $\sim J$ due to the anisotropy of the Hamiltonian. Doping will destroy this order and lead either to a disordered orbital liquid, or may generate a new kind of ordered state which optimizes the kinetic energy of the holes. To investigate this question for an anisotropic model it is in general not sufficient to calculate simply e.g. the correlation function $\langle T_i^z T_j^z \rangle$ defined with respect to the original orbital basis, because the relevant occupied and unoccupied orbitals may be different from the original orbital basis chosen. In the following we therefore introduce a local orthogonal transformation of the orbitals on different sublattices by angles ϕ and ψ , respectively. On the A-sublattice:

$$\begin{aligned} |\tilde{z}\rangle &= \cos(\phi)|z\rangle + \sin(\phi)|x\rangle \\ |\tilde{x}\rangle &= -\sin(\phi)|z\rangle + \cos(\phi)|x\rangle, \end{aligned} \quad (21)$$

and a similar rotation with angle ψ on the B-sublattice. This amounts to new operators, e.g.

$$\tilde{T}_i^z = \cos(2\phi)T_i^z + \sin(2\phi)T_i^x \quad (22)$$

$$\tilde{T}_{i+R}^z = \cos(2\psi)T_{i+R}^z + \sin(2\psi)T_{i+R}^x \quad (23)$$

and new correlation functions, e.g. $\langle \tilde{T}_i^z \tilde{T}_j^z \rangle$ is defined as

$$\begin{aligned} \langle \tilde{T}_i^z \tilde{T}_{i+R}^z \rangle &= \cos(2\phi)\cos(2\psi)\langle T_i^z T_{i+R}^z \rangle + \sin(2\phi)\sin(2\psi)\langle T_i^x T_{i+R}^x \rangle \\ &\quad + \cos(2\phi)\sin(2\psi)\langle T_i^z T_{i+R}^x \rangle + \sin(2\phi)\cos(2\psi)\langle T_i^x T_{i+R}^z \rangle \end{aligned} \quad (24)$$

The angles ϕ and ψ are now chosen such that the nearest neighbor correlation function $\langle \tilde{T}_i^z \tilde{T}_j^z \rangle$ takes a maximal (ferromagnetic) value. With this convention the orbital order is specified by the corresponding local quantization axis, that is by the values of the rotation angles ϕ and ψ . We call this the *optimized orbital basis* (OOB).²¹

In the undoped 2D case (x-y plane) these angles are $\phi = 45^\circ$ and $\psi = 135^\circ$ corresponding to an $\frac{1}{\sqrt{2}}(|x\rangle + |z\rangle)$ and $\frac{1}{\sqrt{2}}(|x\rangle - |z\rangle)$ order at low temperatures (see Fig. 11 and 12). $\langle \tilde{T}_i^z \tilde{T}_{i+R}^z \rangle$ takes a value only slightly smaller than 0.25 at low temperature (Fig. 13), which implies that quantum fluctuations are small in this state. Hence the orbital correlation function $\langle \tilde{T}_i^z \tilde{T}_{i+R}^z \rangle$ of the undoped orbital model is *alternating* (i.e. antiferromagnetic in the pseudo-spin language for the orbital degrees of freedom). That the AF-order seems to be established at a finite temperature for the small clusters means that the correlation length ξ gets larger than the system size L . At small temperatures the correlation functions have about the same value independent of R , i.e. the data shows no spatial decay. Above $T/t = 0.1$ the orbital correlations are small and show a pronounced spatial decay, which can be considered as a signature of a thermally disordered orbital liquid state.

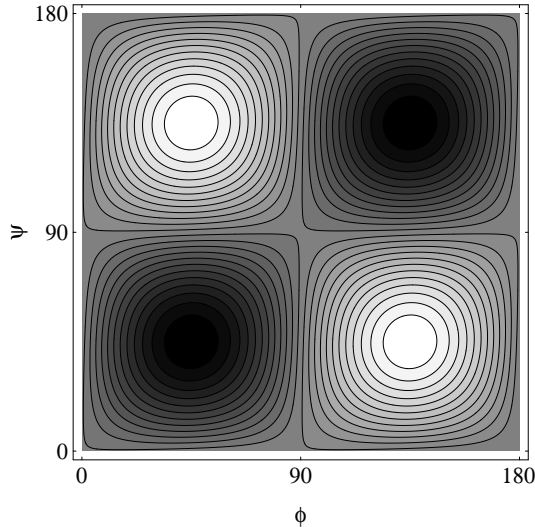


Figure 11: Contourplot of the *rotated* nearest neighbor orbital correlation function $\langle \tilde{T}_i^z \tilde{T}_{i+R}^z \rangle$, $R=(1,0)$, as function of the angles ϕ and ψ for a $N=10$ site planar cluster with $N_e=10$ electrons, $J=0.25t$ ($U=16t$) and $T=0.01t$. White regions correspond to positive (ferromagnetic) and black areas to negative (antiferromagnetic) correlation functions, i.e. $\langle \tilde{T}_i^z \tilde{T}_{i+R}^z \rangle > 0.23$ (< -0.23), respectively. The 25 contour lines are chosen equidistant in the interval $[-1/4, +1/4]$. (From Horsch, Jaklič and Mack²¹)

Experimentally the coexistence of antiferromagnetic (or staggered) orbital order and ferromagnetic spin order has been established in the low-doping regime of LaMnO_3 .^{42,43} It should be recalled that LaMnO_3 has an A-type antiferromagnetic spin structure,⁴⁴ where ferromagnetic layers are coupled antiferromagnetically along the c -axis. In the orbital ordered case the MnO_6 octahedra are deformed, and Mn $3d_{3x^2-r^2}$ and $3d_{3y^2-r^2}$ orbitals with orientation along the x - and y -axis, respectively, have been considered as relevant occupied orbitals.^{45,46} For the planar model we find here the alternate occupation of $\frac{1}{\sqrt{2}}(|x\rangle - |z\rangle)$ and $\frac{1}{\sqrt{2}}(|x\rangle + |z\rangle)$ orbitals (Fig. 12) which are also oriented along the x - and y -axis, however they differ with respect to their shape (and have pronounced lobes along z).

Doping of two holes in a ten site cluster is sufficient to remove the alternating orbital order and establishes a ferromagnetic orbital order ($\phi = \psi = 0$) as can be seen from Figs. 14 and 16. This corresponds to preferential occupation of orbitals with symmetry $x^2 - y^2$ as shown in Fig.15. The pseudospin alignment can be considered as a kind of *double exchange mechanism in the orbital sector*. An interesting feature in Fig.16 for the doped case is the fact that the correlations do not show significant spatial decay even at higher temperatures where the correlations are small. Moreover the correlations in the doped case appear to be more robust against thermal fluctuations than in the undoped case. The characteristic temperature (determined from the half-width in Figs.13 and 16) is $T^* \sim 0.2t$ for the 2-hole case while for the undoped system $T^* \sim 0.05t$. This trend is consistent with the fact that in the doped case order is induced via the kinetic energy and the corresponding scale t is larger than $J = 0.25t$. Although a more detailed analysis would be necessary to account properly for the doping dependence.

It has been shown recently by Ishihara *et al.*²⁹ that in the layered manganite compounds hydrostatic pressure leads to a stabilization of the x^2-y^2 orbitals as well.

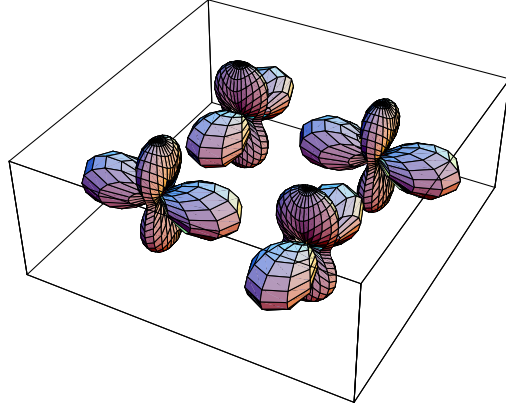


Figure 12: Alternating $\frac{1}{\sqrt{2}}(|x\rangle + |z\rangle)$ and $\frac{1}{\sqrt{2}}(|x\rangle - |z\rangle)$ orbital order in the undoped planar system.

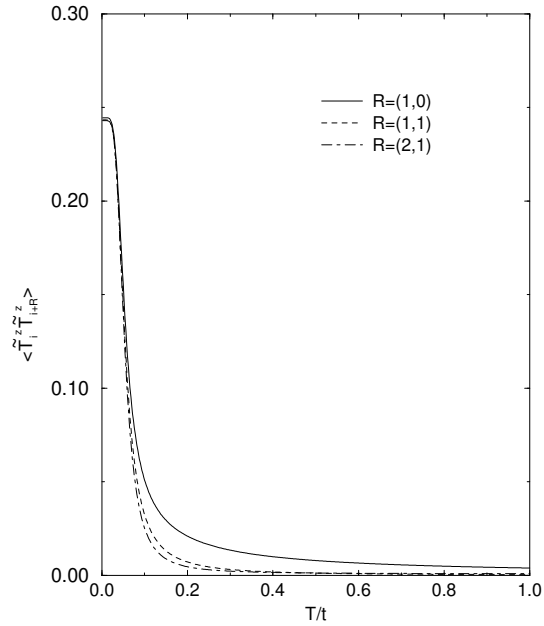


Figure 13: Temperature dependence of $\langle \tilde{T}_i^z \tilde{T}_{i+R}^z \rangle$ with $\phi = 45^\circ$ and $\psi = 135^\circ$ for nearest-neighbors and $\psi = 45^\circ$ for next-nearest neighbors, respectively. Results are shown for different distances R for an undoped $N = 10$ site planar cluster. Parameters as in Fig.11. The strong increase for $T/t \leq 0.1$ is due to the onset of alternating orbital order. (From Horsch, Jaklic and Mack²¹)

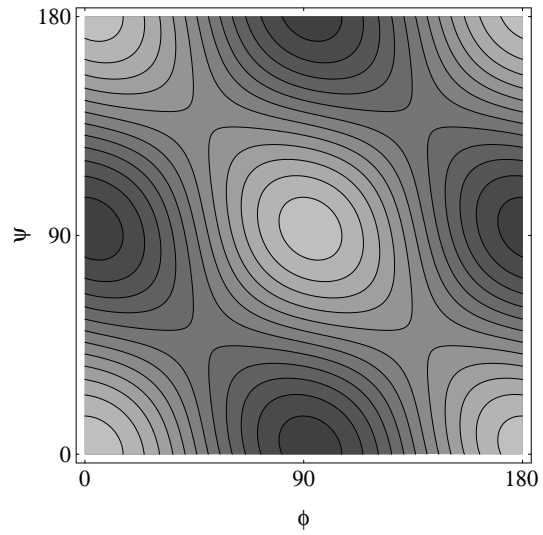


Figure 14: Contourplot of $\langle \tilde{T}_i^z \tilde{T}_{i+R}^z \rangle$ for $R = (1, 0)$ as function of angles ϕ and ψ for a $N=10$ site cluster with two holes. Otherwise same parameters as for Fig.11.

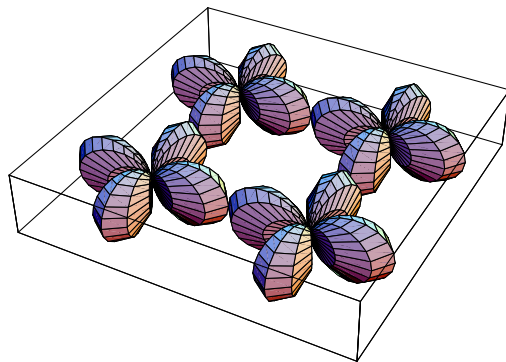


Figure 15: x^2-y^2 orbital order in the doped phase.

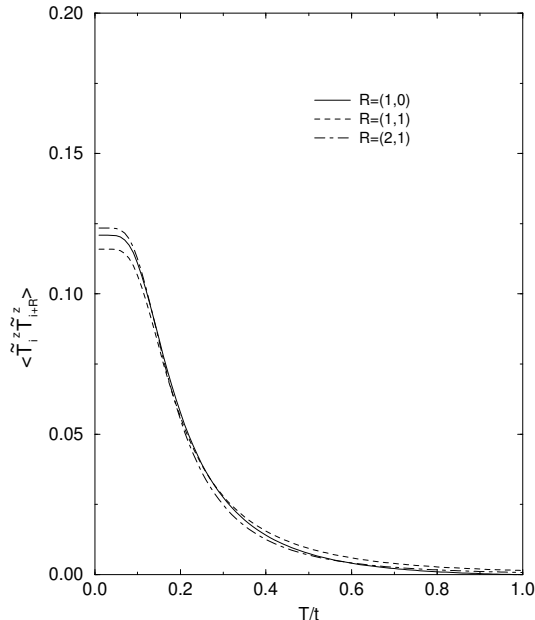


Figure 16: Temperature dependence of $\langle \tilde{T}_i^z \tilde{T}_{i+R}^z \rangle$ with $\phi = 0^\circ$ and $\psi = 0^\circ$ for a 10-site cluster with two e_g holes. Parameters as in Fig.11. The strong increase below $T/t = 0.3$ signals the onset of x^2-y^2 orbital order in the planar model.

A comparison of the doping dependence of spatial correlations with the t - J model is given in Fig.17. In the undoped case the orbital model shows almost classical (orbital) Néel order, whereas in the t - J model correlations are strongly reduced by quantum fluctuations. The $T = 0$ correlation function of the t - J model shows long-range order (LRO) consistent with a strongly reduced sublattice magnetization $m_z \sim 0.3$ (in the thermodynamic limit).

In the orbital model the effect of the two holes ($x = 0.125$ and 0.2) is strong enough to induce ferromagnetic (orbital) correlations, i.e. with a preferred occupation of x^2-y^2 orbitals. In the t - J model instead spin-correlations decay rapidly for two holes on a 20-site cluster ($x = 0.1$), which is consistent with the notion of an AF spin-liquid state (see inset Fig.17).

The preference of ferromagnetic orbital order in the doped case is due to the fact that $t^{\alpha\beta}$ depends on the orbital orientation, and $t^{aa} \gg t^{bb}$. One would expect that for sufficiently strong orbital exchange interaction $J = 4t^2/U$ one reaches a point where antiferromagnetic orbital interactions and ferromagnetic correlations due to the kinetic energy are in balance. This quantum critical point between FM and AF orbital order turns out to be at quite large J values. For the two-hole case ($x = 0.2$) we have found that this crossover happens for quite large orbital interaction $J \sim 2$, i.e. at a value about an order of magnitude larger than typical J values in manganite systems.

Before closing this section, we shall explain the different orbital occupancy in the doped and undoped case in more physical terms. The overlap of the two sets of orthogonal e_g orbitals on neighboring sites changes with the angles ϕ and ψ . (1) In the undoped state the direct hopping between the (predominantly) occupied orbitals $\frac{1}{\sqrt{2}}(|x\rangle + |z\rangle)$ and $\frac{1}{\sqrt{2}}(|x\rangle - |z\rangle)$ on neighboring sites is small (Fig.12). The hopping between these occupied orbitals is blocked anyhow because of Pauli's principle. However t^{ab} between an occupied orbital on one site and an unoccupied orbital on a neighbor site is extremal.

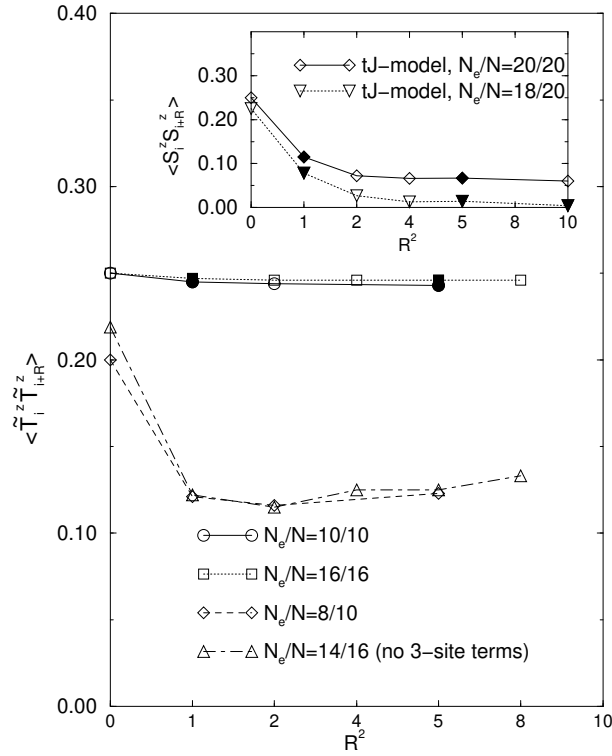


Figure 17: Orbital correlation functions for $T = 0$ as function of distance (squared) for a 10-site and a 4×4 cluster with zero and two holes ($J/t = 0.25$). In the undoped case the correlation function is antiferromagnetic, whereas in the doped case orbital correlations are ferromagnetic. Antiferromagnetic orbital order is indicated by full (negative) and open (positive) symbols, respectively. Inset: The spin correlations $\langle S_i^z S_{i+R}^z \rangle$ for a 20-site 2D Heisenberg model and the t - J model with two holes are shown for comparison (t - J data for $J = 0.4$ taken from Horsch and Stephan⁴⁷). The two-hole case shows a rapid decay of correlations characteristic for an antiferromagnetic spin liquid.

This leads to a maximal antiferromagnetic orbital exchange interaction, and thereby to a lowering of the energy. (2) In the doped case instead, the x^2-y^2 orbital occupancy is preferred on all sites (Fig.15), which implies a large hopping amplitude for holes in the partially occupied x^2-y^2 band, whereas the off-diagonal hopping matrix element t^{ab} and the orbital interactions are reduced for this choice of occupied orbitals. Hence the main energy gain in this case is due to the correlated motion of holes in the x^2-y^2 -band. Nevertheless the off-diagonal hopping plays an important role in the x^2-y^2 ordered state, and leads to the strong incoherent features characteristic for the conductivity $\sigma(\omega)$.

Finally we note that recent experiments by Akimoto *et al.*⁴⁸ proved the existence of an A-type antiferromagnetic metallic ground state in a wide doping concentration regime of the 3D system $(\text{La}_{1-z}\text{Nd}_z)_{1-x}\text{Sr}_x\text{MnO}_3$ and in particular for $\text{La}_{1-x}\text{Sr}_x\text{MnO}_3$ at high doping $x = 0.52 - 0.58$. The latter compound was investigated by Okimoto *et al.* for smaller doping x where the ground state is the uniform ferromagnetic state. The A-type antiferromagnet consists of ferromagnetic layers which are coupled antiferromagnetically. Akimoto *et al.* propose that $x^2 - y^2$ orbitals should be occupied in this state and form a highly anisotropic 2D band. This seems consistent with our finding of $x^2 - y^2$ orbital order in the ferromagnetic planar system where the cubic symmetry is explicitly broken. An experimental study of the optical properties in this concentration regime at low temperature would be particularly interesting.

SUMMARY AND CONCLUSIONS

Our work was motivated by the experimental study of the frequency dependent conductivity of $\text{La}_{1-x}\text{Sr}_x\text{MnO}_3$ by Tokura's group.⁶ In particular these experiments show in the saturated low- T ferromagnetic phase a broad incoherent spectrum and at small frequency in addition a narrow Drude peak, which contains only about 20% of the total spectral weight. This experiment by itself shows that *the ferromagnetic metallic state (although fully spin polarized) is highly anomalous*. These features cannot be explained by the standard double exchange model, but require an additional mechanism. The most natural mechanism, one can think of, is the twofold degeneracy of the e_g orbitals.

We have studied the optical conductivity, the charge stiffness and the optical sum rule for an effective Hamiltonian that contains only the e_g -orbital degrees of freedom. This model follows from the more general Kondo lattice model, when the spins are ferromagnetically aligned. The 'orbital t - J model' is expected to describe the low-temperature physics of manganese oxides in the ferromagnetic saturated phase.

Our results for $\sigma(\omega)$ in the 2D orbital disordered regime show that these characteristic features follow from the orbital model. We believe that the optical conductivity in the 2D orbital liquid regime ($T > T^*$) can be compared with the conductivity in the 3D-orbital liquid state. In particular there is (1) a broad continuum which decreases towards high frequency with a half-width $\omega_{1/2} \sim 2.5$ and $3.5t$ in two and three dimensions, respectively. (2) The absorption increases with decreasing temperature and (3) the absolute value of the incoherent part of $\sigma(\omega)$ at low frequency and temperature $\sigma_0^{inc} \sim 0.4 \cdot 10^3 (\Omega\text{cm})^{-1}$ has the correct order of magnitude as in Tokura's experiments. (4) Despite this strong incoherence there is a finite Drude peak of about 20% of the total sum rule for small J . (5) The coherent motion and the Drude peak become more pronounced for larger values of J due to the 3-site hopping processes in the model. For the value $J/t = 0.25$ estimated here the relative Drude weight is 40 (20) % in the model with (without) 3-site hopping processes, respectively. (6) The low temperature values

for the DC-conductivity and the resistivity can be estimated by assuming a width Γ for the Drude peak (taken from experiment). The additional scattering processes contributing to Γ are due to impurity or grain boundary scattering, i.e. these are extrinsic scattering processes which are not contained in the orbital model. The important information which follows from the model is the weight of the Drude peak, which together with Γ determines the DC-conductivity.

The relatively small Drude peak in comparison with the incoherent part of $\sigma(\omega)$ clearly indicates that the carrier motion is essentially incoherent. Nevertheless we expect a quasiparticle peak in the single particle Green's function, yet with small spectral weight. Our study of the frequency dependent conductivity shows that the (saturated) ferromagnetic state in the manganites has unconventional transport properties due to the scattering from orbital excitations in combination with the exclusion of double occupancy. A detailed study of the orbital dynamics in the doped system is necessary for a deeper understanding of these issues.

The orbital model resembles the t - J model, which describes the correlated motion of charge carriers in the cuprate superconductors. Yet an important difference is the cubic symmetry of the pseudospin representation of the orbital degrees of freedom. The hopping matrix elements depend on the orbital orientation, and are in general different in the two diagonal hopping channels. Moreover there is also an off-diagonal hopping matrix element, which does not exist at all in the t - J model. At low temperatures ($T < T^* \sim 0.2t$) doping induces (ferromagnetic) x^2 - y^2 orbital order for realistic values for the exchange interaction J in the 2D orbital model. This is in striking contrast to t - J physics in cuprates, where the system changes upon doping from antiferromagnetic long-range order to an antiferromagnetic spin liquid. In both models coherent motion coexists with strong incoherent features.

Our calculations have shown that the orbital mechanism can explain the order of magnitude of the conductivity at low temperature. The orbital degrees of freedom are certainly also important for a quantitative calculation of the colossal magnetoresistance. This is obvious because in the full Kondo lattice model there is a close interplay between orbital and spin degrees of freedom.^{22,23}

We acknowledge helpful discussions with F. Assaad, J. van den Brink, L. Hedin, G. Khaliullin, A. Muramatsu, A. M. Oleś and R. Zeyher.

REFERENCES

1. R. von Helmolt *et al.*, *Phys. Rev. Lett.* **71**, 2331 (1993); K. Chahara *et al.*, *Appl. Phys. Lett.* **63**, 1990 (1993); S. Jin *et al.*, *Science* **264**, 413 (1994); Y. Tokura *et al.*, *J. Phys. Soc. Jpn.* **63**, 3931 (1994).
2. C. Zener, *Phys. Rev.* **82**, 403 (1951); P. W. Anderson and H. Hasegawa, *Phys. Rev.* **100**, 675 (1955); K. Kubo and A. Ohata, *J. Phys. Soc Jpn* **33**, 21 (1972).
3. A. J. Millis, P. B. Littlewood and B. I. Shraiman, *Phys. Rev. Lett.* **74**, 5144 (1995); A. J. Millis, R. Mueller and B. I. Shraiman, *Phys. Rev. B* **54**, 5405 (1996).
4. A. J. Millis, *Nature* **392**, 147 (1998).
5. For a recent experimental review see: A. P. Ramirez, *J. Phys.: Condens. Matter* **9**, 8171 (1997).
6. Y. Okimoto, T. Katsufuji, T. Ishikawa, A. Urushibara, T. Arima and Y. Tokura, *Phys. Rev. Lett.* **75** 109 (1995).
7. Y. Okimoto, T. Katsufuji, T. Ishikawa, T. Arima, and Y. Tokura, *Phys. Rev. B* **55**, 4206 (1997).
8. S. G. Kaplan, U. M. Quijate, H. D. Drew, G. C. Xiong, R. Ramesh, C. Meunon, T. Venkatesan, and D. B. Tanner, *Phys. Rev. Lett.* **77**, 2081 (1996).

9. M. Quijada, J. Cerne, J. R. Simpson, H. D. Drew, K. H. Ahn, A. J. Millis, R. Shreekala, R. Ramesh, M. Rajeswari, and T. Venkatesan, *Phys. Rev. B* **58**, 16093 (1998).
10. K. H. Kim, J. H. Jung, and T. W. Noh, *Phys. Rev. Lett.* **81**, 1517 (1998); K. H. Kim *et al.*, *cond-mat/9804284*.
11. T. Ishikawa, T. Kimura, T. Katsufuji, and Y. Tokura, *Phys. Rev. B* **57**, R8079 (1998) and references therein.
12. N. Furukawa, *J. Phys. Soc. Jpn.* **64**, 2734 (1995), *ibid.* **64**, 3164 (1995).
13. S. Ishihara, M. Yamanaka, and N. Nagaosa, *Phys. Rev. B* **56**, 686 (1997).
14. H. Shiba, R. Shiina, and A. Takahashi, *J. Phys. Soc. Jpn.* **66**, 941 (1997).
15. J. Jaklič, P. Horsch, and F. Mack (unpublished).
16. H. Röder, J. Zang, and A. R. Bishop, *Phys. Rev. Lett.* **76**, 1356 (1996).
17. K. J. von Szczepanski, P. Horsch, W. Stephan, and M. Ziegler, *Phys. Rev. B* **41**, 2017 (1990).
18. W. Stephan and P. Horsch, *Int. J. Mod. Phys. B* **6**, 589 (1992); P. Horsch and W. Stephan, in *The Hubbard Model*, ed. by Dionys Baeriswyl *et al.* (Plenum, New York, 1995), p. 193.
19. P. Horsch and W. Stephan, *Phys. Rev. B* **48**, R 10595 (1993).
20. H. Eskes, A. M. Oleś, M. Meinders, and W. Stephan, *Phys. Rev. B* **50**, 17980 (1994).
21. P. Horsch, J. Jaklič, and F. Mack, *Phys. Rev. B* **59**, 6217 (1999).
22. S. Ishihara, J. Inoue, and S. Maekawa, *Phys. Rev. B* **55**, 8280 (1997).
23. L. F. Feiner and A. M. Oleś, *Phys. Rev. B* **59**, 3295 (1999).
24. J. Jaklič and P. Prelovšek, *Phys. Rev. B* **49**, 5065 (1994); *ibid.* **50**, 7129 (1994); *ibid.* **52**, 6903 (1995).
25. For a review see J. Jaklič and P. Prelovšek, *Adv. Phys.* **49**, 1 (2000).
26. J. C. Slater and G. F. Koster, *Phys. Rev.* **94**, 1498 (1954).
27. K. I. Kugel and D. I. Khomskii, *Sov. Phys. JETP* **37**, 725 (1973).
28. W. A. Harrison, *Electronic Structure and Properties of Solids*, (Freeman, San Francisco, 1980).
29. S. Ishihara, S. Okamoto, and S. Maekawa, *J. Phys. Soc. Jpn.* **66**, 2965 (1997).
30. J. Zaanen and A. M. Oleś, *Phys. Rev. B* **48**, 7197 (1993).
31. C. M. Varma, *Phys. Rev. B* **54**, 7328 (1996).
32. A. H. MacDonald, S. M. Girvin, and D. Yoshioka, *Phys. Rev. B* **37**, 9753 (1988) and references therein.
33. B. S. Shastry and B. Sutherland, *Phys. Rev. Lett.* **65**, 243 (1990).
34. A. Urushibara *et al.*, *Phys. Rev. B* **51**, 14103 (1995).
35. W. Kohn, *Phys. Rev.* **133**, A171 (1964).
36. D. Baeriswyl, J. Carmelo, and A. Luther, *Phys. Rev. B* **16**, 7247 (1986).
37. The same twisted boundary conditions were used for the finite temperature studies in this work. These boundary conditions guarantee a nondegenerate closed-shell ground state.
38. F. Mack and P. Horsch, *Phys. Rev. Lett.* **82**, 3160 (1999).
39. D. Poilblanc and E. Dagotto, *Phys. Rev. B* **44**, 466 (1991).
40. B. F. Woodfield, M. L. Wilson, and J. M. Byers, *Phys. Rev. Lett.* **78**, 3201 (1997).
41. R. Kilian and G. Khaliullin, *Phys. Rev. B* **58**, R11841 (1998).
42. J. B. Goodenough, *Phys. Rev.* **100**, 564 (1955).
43. J. B. Goodenough, in *Progress in Solid State Chemistry*, Vol.5, ed. by H. Reiss (Pergamon, London, 1971).
44. E. D. Wollan and W. C. Koehler, *Phys. Rev.* **100**, 545 (1955).
45. G. Matsumoto, *J. Phys. Soc. Jpn.* **29**, 606 (1970).
46. J. B. A. A. Elemans, B. van Laar, K. R. van der Veen, and B. O. Loopstra, *J. Solid State Chem.* **3**, 238 (1971).
47. P. Horsch and W. Stephan, *Physica C* **185-189**, 1585 (1991).
48. T. Akimoto, Y. Maruyama, Y. Moritomo, A. Nakamura, K. Hirota, K. Ohoyama, and M. Ohashi, *Phys. Rev. B* **57**, R5594 (1998).